

Article

# Study on the FES effects of different sizes of stimulation electrodes and different numbers of stimulation channels

Penghui Lin

School of Microelectronics, University of Science and Technology of China, Hefei 230026, China; lph2018@mail.ustc.edu.cn

## CITATION

Lin P. Study on the FES effects of different sizes of stimulation electrodes and different numbers of stimulation channels. *Molecular & Cellular Biomechanics*. 2025; 22(5): 1757.  
<https://doi.org/10.62617/mcb1757>

## ARTICLE INFO

Received: 3 March 2025  
Accepted: 21 March 2025  
Available online: 26 March 2025

## COPYRIGHT



Copyright © 2025 by author(s).  
*Molecular & Cellular Biomechanics* is published by Sin-Chn Scientific Press Pte. Ltd. This work is licensed under the Creative Commons Attribution (CC BY) license.  
<https://creativecommons.org/licenses/by/4.0/>

**Abstract:** This study aims to investigate the functional electrical stimulation (FES) effects of different sizes of stimulation electrodes and different numbers of stimulation channels. Taking the biceps brachii as the target muscle, four FES electrode configurations were designed, varying in electrode size and stimulation channel number. This study recruited ten healthy subjects. Under each FES electrode configuration, a high (30 Hz)-frequency/low (1 Hz)-frequency alternating stimulation was conducted to collect effective muscle contraction strength data and surface electromyography (sEMG) signals. The effects of different FES electrode configurations on muscle contraction strength were analyzed using fatigue-related indicators, and those on myoelectric activity property involving motion unit (MU) recruitment and muscle fiber conduction velocity (MFCV) were explored by means of sEMG data analysis. Both enlarging stimulation electrode size and increasing the number of stimulation channels delayed muscle fatigue, enhanced motor unit recruitment, and generated stronger muscle contractions at the same current intensity. Enlarging the electrode size is more conducive to recruiting more MUs and enhancing muscle contraction output, while increasing the number of stimulation channels is more conducive to delaying muscle fatigue effects. The research results of this article can provide scientific guidance for clinical doctors to develop personalized FES plans, thereby improving treatment effect.

**Keywords:** functional electrical stimulation; muscle fatigue; motor unit recruitment

## 1. Introduction

Functional electrical stimulation (FES) is a peripheral nerve regulation technique that applies low-intensity electric currents to neuromuscular tissue through electrodes in the skin or directly implanted in the motor nerve to cause involuntary muscle contractions to produce functional movement [1]. FES is commonly used in clinical practice to enhance muscle strength and endurance, as well as to alleviate pain [2–4]. In Purohit et al.'s study [5], 51 hemiplegic patients received FES, and significant improvements in muscle strength were found for both upper limb muscles and lower limb muscles. Purohit et al. reported that ambulatory participants with hemiplegic stroke and moderate to severe motor disorders showed significant improvement in response stability and vertical limb support ability after receiving FES [5]. Moreover, FES was reported to reverse long-term denervation muscle atrophy and dystrophy via increasing myofiber diameter size by more than 50% and regenerating new myofiber [6].

Although the effectiveness of FES has been validated in clinical practice, its potential therapeutic mechanisms for muscle function remain not fully understood. The contraction amplitude and the activation of the reflex pathway are considered to be key factors for the recovery of FES [7,8]. In related research, the changes in muscle

state under FES were mainly studied from the perspectives of muscle contraction strength and myoelectric activity. In terms of muscle contraction strength, studies have found that after being subjected to FES, muscles often experience a rapid muscle fatigue phenomenon [9]. Muscle fatigue can be defined as a reduction in the ability of muscles or muscle groups to generate force following prolonged or intense activity [10]. Chou et al. conducted isometric contraction tests on the quadriceps muscles of 10 healthy adults, recording and analyzing muscle strength responses under different stimulation intensities. They found that peak muscle strength rapidly decreases at the beginning, then gradually decreases, and finally stabilizes [11]. Long-term muscle fatigue can damage muscle performance, reduce neuromuscular coordination, and ultimately decrease therapeutic efficacy [12].

In terms of monitoring myoelectric activity during FES, signals collected from the skin are called evoked electromyography (eEMG). Researches have demonstrated that eEMG showed characteristic changes in response to electrical stimulation. Specifically, eEMG is composed of characteristic waveforms called M-waves, which represent the sum of action potentials synchronously triggered by recruited motor units [13]. Researchers explored the effects of FES by analyzing the relevant characteristics of eEMG. For instance, De Marchis et al. measured the peak-to-peak value of M-waves to find the optimal stimulation pattern for eliciting functional hand opening [14]. Li et al. developed a closed-loop FES system using eEMG for real-time control of muscle activation in SCI patients [15]. Additionally, eEMG can reflect changes in muscle fiber conduction velocity (MFCV) and the motor unit recruitment ability. The increase in MFCV and the number of recruited motor units are believed to enhance the therapeutic effects of FES [16,17].

In clinical practice, in order to improve the therapeutic efficacy of FES, it is necessary to scientifically design an FES protocol. Gorgey et al. showed that increasing the intensity of the stimulation current leads to a proportional increase in the size of the muscle cross-sectional area [18]. Vromans et al. assessed the decline in maximum voluntary contraction (MVC) force overtime in muscles with different ratios of fast-twitch and slow-twitch fibers (abductor pollicis brevis (APB) and vastus lateralis (VL)) when activated by FES at three frequencies (10 Hz, 35 Hz, and 50 Hz). They found that at 35 Hz and 50 Hz, the fast-twitch dominant VL exhibited a more rapid decline in contraction force compared to the slow-twitch APB, while no significant difference was observed at 10 Hz, indicating muscles with different muscle fiber components have different sensitivity to different stimulation frequencies [19]. Bergquist et al. optimized the sensory volley induced by electrical stimulation to exploit the mechanisms inherent to the neuromuscular system, thereby enhancing the efficacy [8]. RaviChandran et al. proved that electrode geometry and its potential current distribution are very important for selectivity and comfort [20].

In addition to stimulation current intensity, frequency, and waveform, stimulation location and the size and number of stimulation electrodes should also be considered to improve the therapeutic efficacy of FES. Bickel et al. found that electrical stimulation recruits MUs in a non-selective, spatially fixed, and temporally synchronized manner and pointed out that activating only motor units at fixed positions in the targeted muscle is more likely to be detrimental to muscle functional activity and metabolism [21]. For this reason, some studies developed a spatially

distributed sequential stimulation strategy (SDSS), utilizing multiple surface electrodes to sequentially alter the stimulation region [22,23]. Ye et al. conducted a study on 15 healthy subjects, stimulating their quadriceps and hamstrings using the SDSS scheme and single electrode stimulation (SES) scheme while they performed rowing exercises [24] and found that SDSS can extend rowing time by approximately 30%.

As for the FES electrode, the size typically ranges from 2 to 20 cm<sup>2</sup> in clinical applications, with adjustments made according to the size of the target muscle and patients' subjective feedback. Generally, smaller electrodes (2–5 cm<sup>2</sup>) are used for small muscle groups, while larger electrodes (10 cm<sup>2</sup> or larger) are employed for larger muscle groups. It is generally believed that smaller electrodes provide more precise stimulation, while larger electrodes disperse the stimulation energy and reduce discomfort. Flodin et al. conducted a study on 15 healthy subjects using electrodes of three different sizes for electrical stimulation [25]. They found that optimizing electrode size and selecting appropriate positions in the quadriceps, hamstring, and gluteal muscles are crucial for achieving the desired comfort and intensity. Regarding the number of stimulation electrodes, multi-channel stimulation is typically applied in scenarios requiring multiple muscle functional reconstructions [26,27]. In summary, there is a lack of systematic research and valuable research results on the effects of different-sized stimulation electrodes or different channel stimuli on muscle contraction strength or the myoelectric property of target muscles. In order to provide a scientific basis for the selection of electrode size and channel in clinical FES treatment, this study aims to reveal the effects of different sizes of stimulation electrodes and different numbers of stimulation channels on muscle contraction strength and myoelectric activity. Taking the biceps brachii as the target muscle, the main contributions and innovations can be summarized as follows: 1) four FES electrode configurations with different electrode sizes and channels were designed; 2) a high-frequency/low-frequency alternating stimulation experiment protocol was designed and conducted to obtain effective muscle contraction strength data and eEMG data; 3) the effects of different FES electrode configurations on muscle contraction strength were analyzed using fatigue related indicators, and that on myoelectric activity property including motion unit (MU) recruitment ability and MFCV were explored by means of eEMG data analysis; 4) Based on the research results, recommendations have been provided for the selection of electrode size and stimulation channel for clinical FES treatment. The research results of this paper are of great significance for promoting the clinical application of FES technology.

## **2. Methodology**

With the goal to investigate the effects of stimulation electrode size and channel quantity on the muscle contraction strength and myoelectric activity of the target muscle, as illustrated in **Figure 1**, the research framework consists of three main parts. The first part is the design of four FES electrode configurations and the high-frequency/low-frequency alternating stimulation protocol. The purpose of designing a stimulation protocol is to collect effective muscle strength data and eEMG data for subsequent analysis. The second part is FES data collection, involving recruiting

subjects, carrying out FES experiments with different electrode configurations, and collecting muscle force data and eEMG data. The third part is data processing and analysis to explore the variations in muscle contraction strength and myoelectric activity under FES with different electrode configurations.

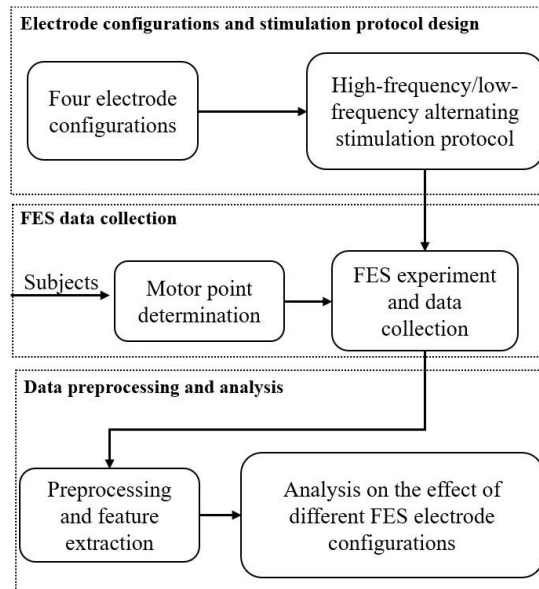


**Figure 1.** The research framework.

## 2.1. Subjects and devices

This study was approved by the Biomedical Ethics Committee of the University of Science and Technology of China (No. 2022-N(H)-150). Ten subjects (six men and four women aged between 22 and 25 years) with no history of neuromuscular or metabolic disorders were recruited from the School of Microelectronics, University of Science and Technology of China (**Table 1**), and each subject signed an informed consent form.

**Table 1.** Participant demographics.

Participant	Age	Height (cm)	Weight (kg)	Sex
1	23	185	78.2	M
2	24	173	68.4	F
3	24	172	74.0	M
4	24	180	76.3	M
5	23	164	55.9	F
6	24	163	51.4	F
7	24	162	53.3	F
8	25	174	71.2	M
9	25	181	70.5	M
10	25	176	68.8	M

A programmable four-channel neuromuscular electrical stimulator as shown in **Figure 2a** (ENS001, Nanochap, China) was used for electrical stimulation. It supports

up to 4 electrical stimulation channels with adjustable parameters, including current ranging from 33  $\mu\text{A}$  to 67 mA, frequency ranging from 1 to 250 KHz, and three waveforms (square, sine, and triangular) to choose from and is connected to a computer via an emulator. The stimulation electrodes (as shown in **Figure 2b**) used are commercially available disposable self-adhesive electrodes. The positive electrode has two sizes: One is a small round electrode (SRE) with a radius of 1.25 cm covering an area of 4.9  $\text{cm}^2$ , and the other is a large square electrode (LSE) with a size of  $5 \times 2 \text{ cm}^2$ . The negative electrode of the stimulation electrode has only one size that is the same as LSE.

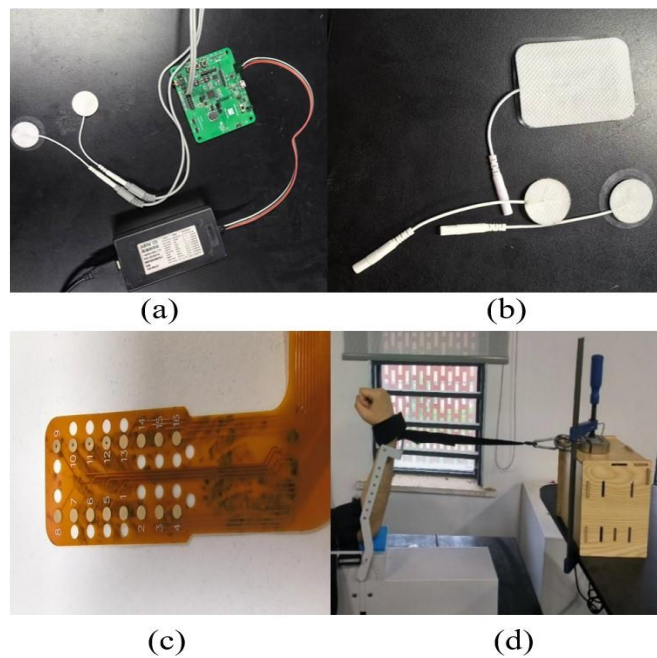


**Figure 2.** Components of the experimental system and experimental setup **(a)** electrical stimulator and emulator; **(b)** stimulation electrodes; **(c)** HD-sEMG grid; **(d)** experimental setup.

The data acquisition equipment consists of three main parts: a force sensor (LAS-B, Norson, China), a self-developed 16-channel HD-sEMG grid (size:  $8 \times 2$ ; area:  $5 \text{ cm} \times 3 \text{ cm}$ ; diameter: 3 mm; inter-electrode horizontal distance: 15 mm; vertical distance: 6 mm) as shown in **Figure 2c**, and a 128-channel signal collector. The gain of the amplifier of HD-sEMG signals is 1371. Force and SEMG signals were recorded simultaneously at a sampling frequency of 2000 Hz using a 16-bit A/D converter (ADS1198).

## 2.2. FES electrode configurations and the stimulation protocol

Taking the biceps brachii as the target muscle, as shown in **Figure 3**, four FES electrode configurations were designed, including a single-channel round electrode scheme (SCES), a dual-channel round electrode scheme (DCES), a triple-channel round electrode scheme (TCES), and a single-channel square electrode scheme (SSES). To ensure that current can efficiently propagate along the biceps fibers and maximize the muscle activation, the positive electrode was placed at the motor point of the belly, and the negative electrode was placed near the elbow joint. The motor

point was defined as the area that elicits maximal muscle contraction. The motor point along with each subject's maximum tolerable current was determined through repeated trials prior to formal experiments. As shown in **Figure 3**, for SCES, an SRE was placed at the center of the motor point as a positive electrode; for DCES, two SREs were placed side by side on the motor point; for TCES, three SREs were placed side by side on the motor point; for SSES, an LSE was placed at the motor point. The 16-channel HD-sEMG grid was placed between the positive and negative electrodes of the stimulation electrode. In **Figure 3**, P represents positive electrode, N represents negative electrode, and G represents HD-sEMG grid.

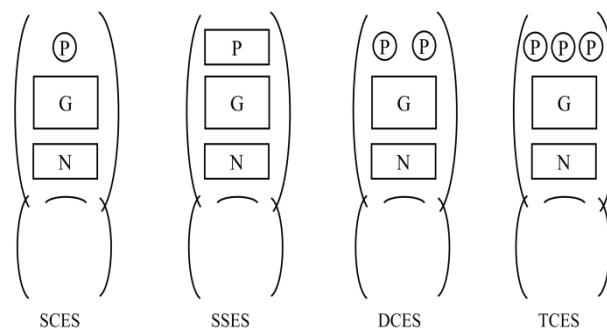


**Figure 3.** The placement of stimulation electrodes and HD-sEMG grid under the four FES electrode configurations.

In order to analyze the muscle contraction strength and myoelectric activity property under FES, it is necessary to use appropriate current intensity and stimulation frequency to obtain effective muscle contraction force data and eEMG data. From a safety perspective, the stimulation current intensity of SCES and SSES was set to subjects' maximum tolerable current. For DCES and TCES, the current intensity of each channel was half and one-third of the maximum tolerable current, respectively. In most clinical rehabilitation treatments and related studies, the stimulation frequency of FES is usually set between 20 and 50 Hz. Lower frequencies of FES (1 to 20 Hz) are used to enhance muscle endurance and venous blood flow [3,28–30]. Previous studies have shown that different muscle fiber types respond differently to varying stimulation frequencies. Specifically, low-frequency stimulation can recruit more slow-twitch, fatigue-resistant Type I fibers, while high-frequency stimulation can recruit more fast-twitch, easily fatigued Type II fibers [10,31].

To investigate the electrical activity property of motor units composed of different types of muscle fibers in the biceps brachii muscle (which is composed of 50–70% Type II fibers [32]), a high-frequency (30 Hz)/low-frequency (1 Hz) alternating stimulation protocol was designed. The 30 Hz high-frequency stimulation mode consisting of symmetric biphasic pulses with a duty cycle of 0.1 was carried out to recruit Type II MU. Each high-frequency stimulation cycle lasted for 3 s. Under high-frequency stimulation, the muscle contracted periodically and produced isometric contractile force. The 1 Hz low-frequency stimulation mode consisting of two symmetric biphasic pulses with a duty cycle of 0.1 was adopted to recruit Type I MU. The duration of each low-frequency stimulation cycle was 2.5 s. Under low-frequency stimulation, the muscle only experienced slight twitches when pulses arrived and remained relaxed the rest of the time, preventing additional muscle fatigue.

It is worth noting that under 30 Hz high-frequency stimulation, when the duration of the M-wave exceeds the reciprocal of the stimulation frequency, M-wave truncation occurs, making it difficult to use the M-wave feature for electrical activity analysis. However, the collected eEMG signal contains complete M-waves under 1 Hz low-frequency stimulation.

### 2.3. FES experimental setup and data collection

For each subject, FES data collection experiments were conducted under the four electrode configurations with intervals of at least 24 h. The subjects underwent repeated electrical stimulation tests one day before the first data collection experiment to determine their maximum tolerated current and motion point. During the FES data collection experiment, as shown in **Figure 2d**, subjects sat in a comfortable chair with their right arm secured using a fixture, maintaining the upper arm horizontally and the forearm vertically. The HD-sEMG grid and self-adhesive electrodes were fixed to the biceps brachii with extra elastic bandages. The wrist was connected horizontally to the force sensor using an inelastic strap to measure isometric contraction force (ICF).

**Figure 4** shows the experimental timeline. At first, subjects attempted two maximum isometric contractions (MIC) with their biceps brachii, each lasting 1–2 s, with a 30-s interval between the two attempts. When the difference between the two attempts exceeded 10%, a third attempt was made. After a 2-min rest period, the electrical stimulation protocol was executed. The 30 Hz high-frequency stimulation mode and the 1 Hz low-frequency stimulation mode alternated for 10 min, or stopped when ICF values detected under 10 consecutive high-frequency stimuli remained unchanged. To ensure that muscle fatigue was entirely caused by electrical stimulation, subjects were required not to exert force actively during the FES period. ICF and eEMG signals were simultaneously recorded and also displayed in real-time on a computer screen for observation by the experimental operator.

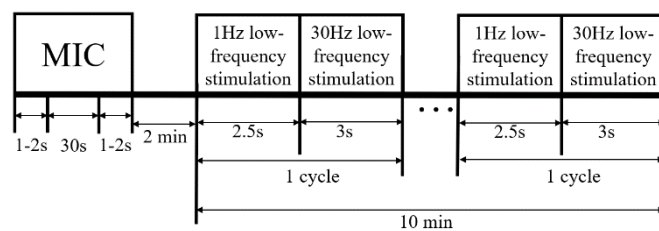


**Figure 4.** The experimental timeline.

### 2.4. Data processing and analysis scheme

In order to analyze the muscle contraction property and myoelectric activity property under FES, the three types of data collected were analyzed as shown in **Figure 5**. The first type is an ICF signal collected under 30 Hz high-frequency stimulation, which can reflect the changes in muscle contraction strength and demonstrate the muscle fatigue property. The second type is an eEMG signal collected under 30 Hz high-frequency stimulation, whose time-varying amplitude and frequency features can display changes in the number of recruited Type II MU and MFCV. The third type is an eEMG signal collected under 1 Hz low-frequency stimulation, whose

amplitude features can be used to assess the recruitment of Type I MU. Below, we will introduce the processing and analysis methods for these three types of data separately.

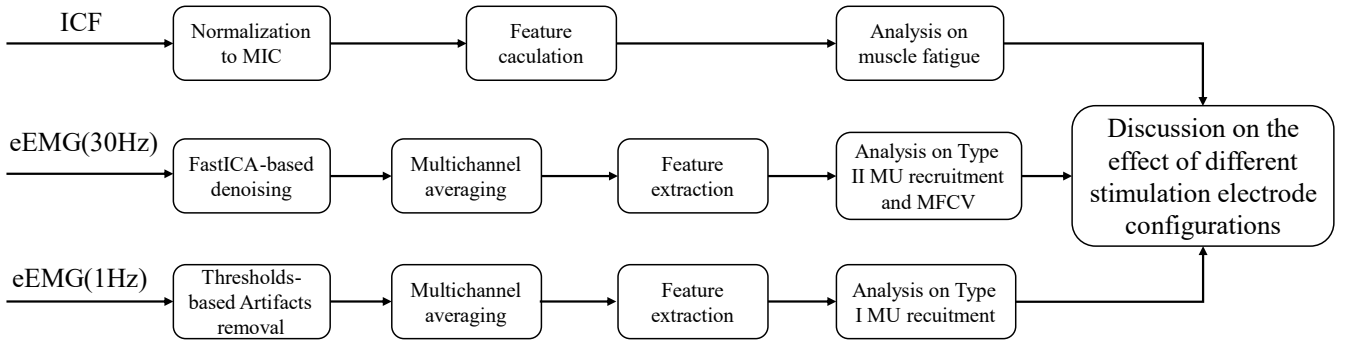


**Figure 5.** The flowchart of the data processing and analysis.

#### 2.4.1. ICF data collected under 30 Hz high-frequency stimulation

ICF signals were used to analyze muscle contraction property, especially the muscle fatigue phenomenon. The average value of ICF during one cycle of 30 Hz high-frequency stimulation was calculated firstly and then was normalized to MIC to eliminate individual differences. MIC was the average value of the two maximum isometric contraction forces at the beginning of each experiment. Based on the average ICF values, two indicators were calculated to characterize muscle fatigue property. The first indicator is fatigue time (FT), defined as the time required for ICF to decrease by 50% or 75% of the initial value corresponding to the first cycle. The former is called 50% FT, and the latter is called 75% FT. The selection of these two time points was based on the property of the experimental data. During the experiment, we found that muscle contraction strength initially decreases rapidly, then slows down and eventually stabilizes. For most subjects, 50% FT falls within the range where the decline rate of muscle strength begins to slow down, while 75% FT is generally within the stable range. The second indicator is fatigue time integral (FTI), defined in Equation (1), representing the integral of the normalized force curve from the beginning to the fatigue time. Corresponding to 50% FT and 75% FT, respectively, there are two FTI parameters, namely 50% FTI and 75% FTI. In this study, we understood the muscle fatigue process and changes in muscle contraction levels by analyzing FT and FTI values. At the same time, using subject and electrode configuration as fixed factors, a two-factor analysis of variance (ANOVA) was conducted on FT and FTI to explore whether different electrode configurations have significantly different muscle fatigue properties and whether there are individual differences.

$$FTI = \int_0^{FT} ICF(t)dt \quad (1)$$

#### 2.4.2. eEMG data collected under 30 Hz high-frequency

For eEMG signals collected under 30 Hz high-frequency stimulation, a FastICA-based denoising method was applied for removing stimulation artifacts firstly [33]. Stimulus artifacts refer to the voltage effect generated by current pulses passing through subcutaneous tissue, which has high amplitude characteristics compared to

eEMG signals generated by MU recruitment. The FastICA algorithm was applied to decompose 16-channel HD-sEMG signals into 16 components firstly; then the two components with the largest amplitude were identified and abandoned as noise, and the remaining components were reconstructed to obtain denoised eEMG signals. In order to reflect the overall response of the biceps brachii to electrical stimulation, 16-channel denoised signals were averaged to obtain a single-channel denoised eEMG signal, then the root mean square (RMS) and mean frequency (MNF) of each stimulation cycle were calculated. As defined in Equation (2), RMS is commonly used to describe the variations in amplitude of EMG signals and is believed to increase with the recruitment of Mus [34,35]. MNFs are defined by Equation (3) and can reflect changes in power spectrum, believed to decrease with MFCV decreasing [36,37].

To explore the changes in recruitment of Type II MUs and MFCV under different electrode configurations, we conducted a phased analysis on the changes in RMS and MNF in relation to the stimulation time of FES, based on the aforementioned two fatigue time points. Specifically, the (0–50%) FT period corresponds to the rapid decline phase of muscle strength, and the (50%–75%) FT period corresponds to the phase where the decline rate slows and eventually stabilizes. Firstly, the least squares method was used to linearly fit the segmented curves of RMS and MNF over time, obtaining four feature change rates (CRs) in the two time periods of (0–50%) FT and (50%–75%) FT, named as  $CR_{RMS} (0-50)\%$ ,  $CR_{RMS} (50-75)\%$ ,  $CR_{MNF} (0-50)\%$ , and  $CR_{MNF} (50-75)\%$ , respectively. Then, the relative changes (RCs) of RMS and MNF at the fatigue points of 50% FT and 75% FT relative to the start of the stimulus were calculated and named as  $RC_{RMS} (0-50)\%$ ,  $RC_{RMS} (0-75)\%$ ,  $RC_{MNF} (0-50)\%$ ,  $RC_{MNF} (0-75)\%$  respectively. The change rates reflect the speed at which the features vary with FES stimulation time, while the relative changes indicate the magnitude of the variation. Based on the extracted feature data, a two-factor analysis of variance (ANOVA) was conducted to explore whether different electrode configurations have significantly different effects on Type II MU recruitment and MFCV under the 30 Hz high-frequency stimulation and whether there exist individual differences.

$$RMS = \sqrt{\frac{\sum_{n=1}^N y_n^2}{N}} \quad (2)$$

$$MNF = \frac{\sum_{n=1}^N f_n \cdot P(f_n)}{\sum_{n=1}^N P(f_n)} \quad (3)$$

where  $y_n$  refers to the denoised eEMG signal at sample  $n$ ,  $f_n$  corresponds to the  $n^{th}$  frequency bin of the STFT, and  $P(f_n)$  refers to the power at  $f_n$ .

#### 2.4.3. eEMG data collected under 1Hz low-frequency stimulation

The eEMG signals under low-frequency stimulation are mainly composed of electrical stimulus artifacts and complete M-waves. Typically, an electrical stimulus artifact is a pulse lasting a few milliseconds, whereas an M-wave lasts longer, rises and falls more slowly, and has a smaller amplitude than an artifact. In order to extract complete M-waves, this study employed a threshold-based method to remove stimulation artifacts, referring to the research of de Sousa et al. [38]. In this method, the position of an electrical stimulus artifact was located firstly, and the endpoint of

the electrical stimulus artifact was considered as the starting point of an M-wave. Then, a 0.2 s signal was extracted as the M-wave. Since the second derivative can accurately locate and amplify regions with more pronounced signal changes, thresholds were defined as Equations (4) and (5).

$$Th1 = \frac{\overline{d^2x}}{dt^2} + \sigma_d \quad (4)$$

$$Th2 = \frac{\overline{d^2x}}{dt^2} - \sigma_d \quad (5)$$

where  $\frac{\overline{d^2x}}{dt^2}$  and  $\sigma_d$  are the mean value and standard deviation of the second derivative of the eEMG signal. When the amplitude of the second derivative of the signal was greater than the upper threshold ( $Th1$ ) or less than the lower threshold ( $Th2$ ), it was marked as a stimulus artifact.

M-wave is composed of the synchronized sum of all muscle fiber action potentials induced by electrical stimulation [13]. Rodriguez-Falces et al. found that the amplitude of the M-wave can reflect the change in the transmembrane potential, especially the amplitude of the monopolar M-wave is proportional to the number of motor units recruited [39,40]. Therefore, the positive amplitude of the M-wave (M-PA) relative to the baseline was adopted as the amplitude feature in this study. Specifically, the 16-channel signals for each stimulation cycle were averaged to get a single-channel signal before feature extraction. Due to the 1 Hz low-frequency stimulation cycle containing two square waves, two complete M-waves can be generated. Then, the average of the two M-PA values was calculated for each cycle. Similarly, the change curve of M-PA over time was fitted with the least squares method in a piecewise linear manner, and the change rates in the periods of (0–50%) FT and (50%–75%) FT were calculated and named as  $CR_{M-PA}$  (0–50)%,  $CR_{M-PA}$  (50–75)%, respectively. Subsequently, the relative changes at the fatigue points of 50% FT and 75% FT relative to the start of the stimulus were calculated and named as  $RC_{M-PA}$  (0–50)%,  $RC_{M-PA}$  (50–75)%, respectively. In order to evaluate the Type I MU recruitment ability of different electrode configurations during a complete experiment, the average value of the M-PA of all M-waves extracted from a single experiment was calculated and named as aM-PA. Similarly, a two-factor analysis of variance (ANOVA) was conducted to explore whether different electrode configurations have significantly different effects on Type I MU recruitment ability and whether there are individual differences.

Data analysis was performed in Matlab R2022b; statistical testing was performed in SPSS 25; post-hoc power calculations were performed in G\*Power.

### 3. Results

#### 3.1. Analysis of muscle fatigue property based on ICF

**Figure 6** shows the ICF curve of a representative subject in the first 5.5 min of FES experiments with the four electrode configurations, where white circles indicate the positions of 50% FT, black dots indicate the positions of 75% FT, and the

corresponding FTI values are shown next to each point. ICFs induced by the four electrode configurations are roughly similar, ranging from 16% to 19% of MIC. At the same time, ICF curves show a similar change trend with an increase in stimulation time, starting to rapidly decline, then slowing down and finally stabilizing. This phenomenon indicates that at the beginning of the four different FES experiments, muscle contraction levels caused by the same intensity of simulation current are roughly equal. As the stimulation time increases, there is a decline in muscle strength caused by rapid fatigue. Further observation reveals that there are certain differences in FT and FTI values among the four electrode configurations. For the representative subject, ICF decreases the fastest under SCES with the smallest FT and FTI values, meaning the fastest muscle fatigue process and the lowest muscle contraction level. For the other three electrode configurations, while the 50% FT points are relatively close, the 75% FT points are far apart from each other, showing that the four electrode configurations cause different muscle fatigue processes. When ICFs reach the stable stage, muscle contraction levels maintained are also different. SCES is the lowest, DCES and TCES are high, and SSES is in the middle.

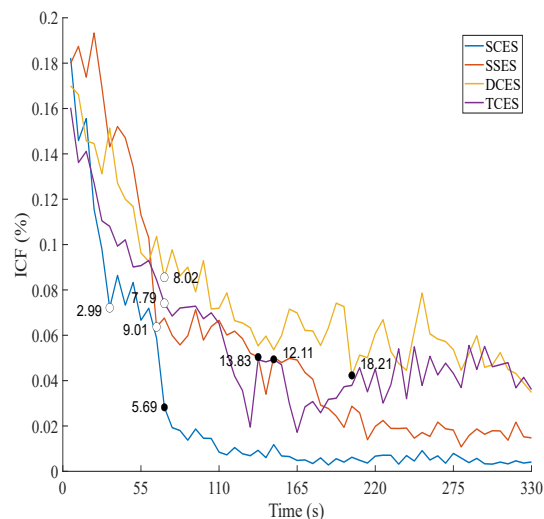


**Figure 6.** ICF curve of a representative subject with the four electrode configurations.

**Table 2** records the average FT and FTI values for all ten subjects. **Table 3** gives the results of the two-factor analysis of variance. In summary, 50% FT values increase in the order of SCES, SSES, DCES, and TCES, and 75% FT values increase in the order of SCES, SSES, TCES, and DCES. The SSES configuration gets the highest 50% FTI and 75% FTI, followed by DCES, TCES, and SCES. There are significant differences ( $p < 0.05$ ) in all four muscle fatigue indicators under different electrode configurations, and there are no individual differences ( $p > 0.05$ ) among subjects. Following the detection of significant differences, post-hoc power analysis was conducted, and the results indicated that the statistical power exceeded 0.8, suggesting that the sample size was sufficiently large to reliably detect the observed effect.

**Table 2.** FT and FTI values (mean ± standard deviation) for ten subjects.

	50% FT (s)	75% FT (s)	50% FTI	75% FTI
SCES	56.0 ± 9.2	106.4 ± 39.0	5.4 ± 1.5	8.01 ± 2.9
SSES	109.6 ± 31.8	195.2 ± 80.1	11.4 ± 4.9	16.6 ± 8.4
DCES	157.6 ± 58.9	253.6 ± 56.3	13.2 ± 6.0	18.2 ± 9.8
TCES	134.4 ± 22.7	242.4 ± 40.6	13.6 ± 5.1	18.9 ± 7.3

**Table 3.** Results of two-factor ANOVA analysis for FT and FTI.

	P-value		$\eta^2$	
	Configuration	Subject	Configuration	Subject
50% FT	0.001	0.098	0.670	0.386
75% FT	0.001	0.407	0.461	0.265
50% FTI	0.003	0.725	0.400	0.183
75% FTI	0.019	0.818	0.304	0.157

**Figure 7** illustrates the results of multiple comparisons regarding electrode size. Specifically, the four indicators of SCES are different from SSES on average, among which 50% FT, 75% FT, 50% FTI, and 75% FTI are significantly ( $p < 0.05$ ) lower than SSES. This result indicates that enlarging the electrode size can slow the muscle fatigue process and enhance muscle contraction level.

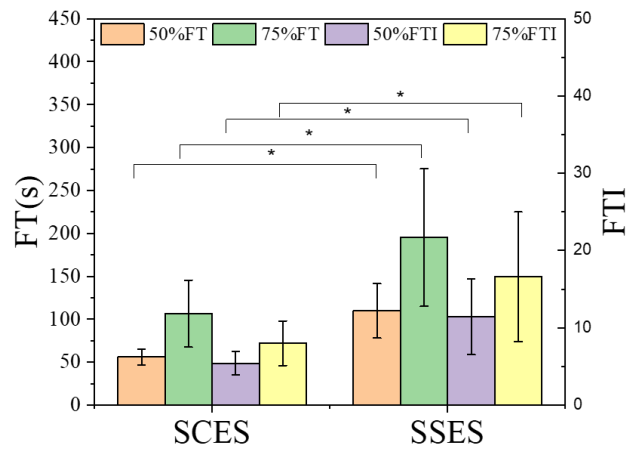


**Figure 7.** Multiple comparison regarding electrode size \* Denotes significance ( $p < 0.05$ ).

**Figure 8** displays the results of multiple comparisons regarding channel number. The 50% FT, 75% FT, 50% FTI, and 75% FTI values of SCES are significantly ( $p < 0.05$ ) lower than those of DCES and TCES. Additionally, there were no significant differences between DCES and TCES ( $p > 0.05$ ). These results indicate that increasing the number of stimulation channels can also reduce the muscle fatigue process and enhance muscle force output. The lack of significant differences between DCES and TCES suggests that further increasing stimulation channels has a limited impact on both slowing the fatigue process and improving muscle contraction level.

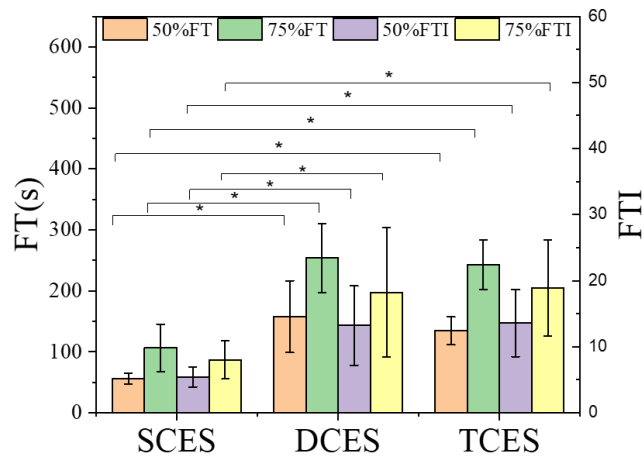


**Figure 8.** Multiple comparison regarding channel number \* Denotes significance ( $p < 0.05$ ).

### 3.2. Analysis of myoelectric property of type II MU

The analysis of myoelectric property Type II MU was carried out on eEMG data collected under 30 Hz high-frequency stimulation. Specifically, MU recruitment property was explored using the RMS feature, and MFCV change was analyzed based on the MNF feature.

#### 3.2.1. Type II MU recruitment property

**Figure 9** shows the RMS curve of a representative subject in the first 5.5 min of FES experiments with the four electrode configurations. Under the four electrode configurations, RMS shows a similar trend of first increasing and then decreasing or remaining stable. This indicates that initial electrical stimulation can induce neural excitability and recruit a certain amount of Type II MU. However, as the stimulation continues, the nervous system's adaptation to repeated electrical stimulation will reduce the recruitment of Type II MU. At the same time, there are significant differences in RMS values obtained under the four different electrode configurations, namely  $SSES > TCES > DCES > SCES$ . **Table 4** records the average  $CR_{RMS} (0-50)\%$ ,  $CR_{RMS} (50-75)\%$ ,  $RC_{RMS} (0-50)\%$  and  $RC_{RMS} (0-75)\%$  values for all 10 subjects. **Table 5** gives the results of the two-factor analysis of variance. By observing **Table 5**, it can be found that electrode configuration has a significant impact on the four RMS change features. Post-hoc power analysis indicated that the statistical power exceeded 0.8. Meanwhile, under the same electrode configuration, the individual differences of the four features are not obvious. From **Table 4**, it can be found that during the period of  $(0-50)\%$  FT, the  $CR_{RMS} (0-50)\%$  of the four electrode configurations are positive. During the period of  $(50-75)\%$  FT, the  $CR_{RMS} (50-75)\%$  of SCES and TCES is positive, while that of the other two configurations is negative. Additionally, the  $RC_{RMS} (0-75)\%$  of SCES is 45.5%, which is greater than the  $RC_{RMS} (0-50)\%$  value of 37.6%. The  $RC_{RMS} (0-75)\%$  of SSSES, DCES and TCES are -4.9%, -2.1%, and -4.4%, all are lower than their corresponding  $RC_{RMS} (0-50)\%$  of 4.7%, 0.6%, and 2.1%.

**Table 4.** The four RMS features for all 5 subjects.

	$CR_{RMS} (0-50)\%$ ( $\mu V/s$ )	$CR_{RMS} (50-75)\%$ ( $\mu V/s$ )	$RC_{RMS} (0-50)\%$ (%)	$RC_{RMS} (0-75)\%$ (%)
SCES	$5.36 \pm 4.92$	$1.66 \pm 4.87$	$37.6\% \pm 35.7\%$	$45.5\% \pm 63.0\%$
SSES	$0.18 \pm 1.09$	$-0.54 \pm 0.96$	$4.7\% \pm 13.0\%$	$-4.9\% \pm 18.1\%$
DCES	$0.04 \pm 1.16$	$-0.44 \pm 0.93$	$-0.6\% \pm 14.3\%$	$-2.1\% \pm 9.4\%$
TCES	$0.58 \pm 1.32$	$0.24 \pm 0.61$	$2.1\% \pm 13.9\%$	$-4.4\% \pm 13.4\%$

**Table 5.** Results of two-factor ANOVA analysis for RMS features.

	<i>P</i> -value		$\eta^2$	
	Configuration	Subject	Configuration	Subject
$CR_{RMS} (0-50)\%$	0.001	0.514	0.456	0.237
$CR_{RMS} (50-75)\%$	0.009	0.692	0.346	0.192
$RC_{RMS} (0-50)\%$	0.001	0.274	0.524	0.305
$RC_{RMS} (0-75)\%$	0.214	0.479	0.150	0.246

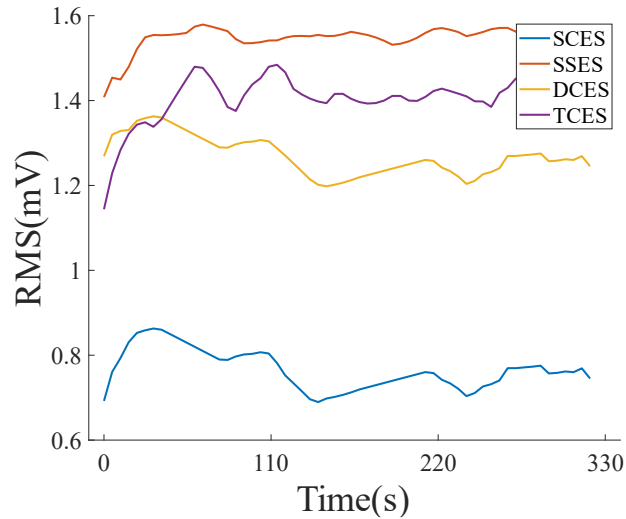


**Figure 9.** RMS curve of a representative subject.

By comparing RMS values of SCES and SSES, we can conclude that enlarging electrode size can enhance the recruitment of Type II MU under 30 Hz high-frequency FES. **Figure 10** illustrates the results of multiple comparisons regarding electrode size. The  $CR_{RMS} (0-50)\%$  for SCES and SSES are 5.36 and 0.18, respectively, and the  $RC_{RMS} (0-50)\%$  are 37.6% and 4.7%, respectively. During the period of (50–75)% FT,  $CR_{RMS} (50-75)\%$  values for the two configurations are 1.66 and  $-0.54$ , respectively, while  $RC_{RMS} (0-75)\%$  values are 45.5% and  $-4.9\%$ , respectively. These results show that, within the period of (0–75)% FT, and type II MU recruitment ability of SCES is increased, while that of SSES firstly increases and then decreases.

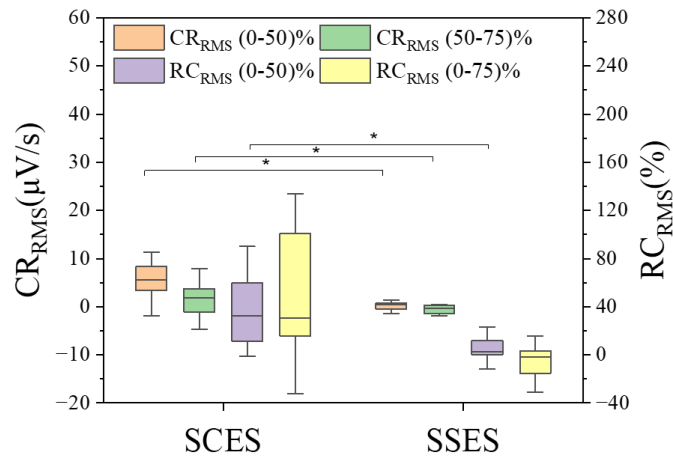


**Figure 10.** Multiple comparison regarding electrode size \* Denotes significance ( $p < 0.05$ ).

By comparing RMS values of SCES, DCES, and TCES, we can conclude that increasing the number of channels can enhance the recruitment of Type II MU under 30 Hz high-frequency FES. **Figure 11** shows the results of multiple comparisons regarding channel number. RMS variations of DCES and TCES have significant differences compared to SCES. The four RMS features of DCES and TCES are all lower than those of SCES, among which  $CR_{RMS} (0-50)\%$ ,  $RC_{RMS} (0-50)\%$  and  $RC_{RMS} (0-75)\%$  have significant differences ( $p < 0.05$ ). Compared to SCES, the RMS of DCES and TCES increases at a slower rate during the period of (0-50)% FT. The above experimental results indicate that the number of Type II MUs recruited by single-channel stimulation shows a relatively high upward trend over time, while the MU recruitment ability of multi-channel electrodes first increases and then decreases. In addition, there is no significant difference between DCES and TCES ( $p > 0.05$ ).

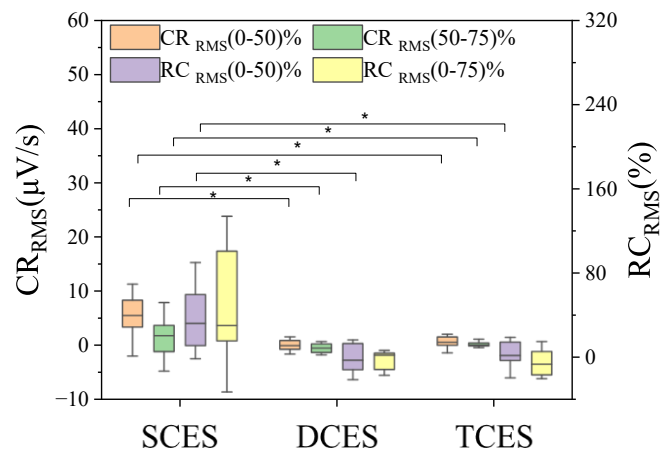


**Figure 11.** Multiple comparison regarding channel number \* Denotes significance ( $p < 0.05$ ).

### 3.2.2. Muscle fiber conduction velocity

**Figure 12** shows the MNF curve of a representative subject in the first 5.5 min of FES experiments with the four electrode configurations. The MFCVs of the four electrode configurations are certainly different, but they have a common downward

trend over time, and eventually stabilize within a certain range. In addition, the MNF of SSES, DCES, and TCES are relatively close, while that of SCES is lower. **Table 6** shows the average  $CR_{MNF}$  (0–50)%,  $CR_{MNF}$  (50–75)%,  $RC_{MNF}$  (0–50)% and  $RC_{MNF}$  (0–75)% values for all the ten subjects, while **Table 7** shows the results of a two-factor analysis of variance. There are no significant differences in the four indicators of MNF ( $p > 0.05$ ) among different configurations ( $p > 0.05$ ) or subjects ( $p > 0.05$ ). The above results indicate that enlarging electrode size or increasing the number of channels will improve MFCV. However, regardless of the electrode configuration, MFCVs will decrease with FES time. When the excitability of the stimulation disappears, the muscle fiber conduction property remains stable, and there is no individual difference in this effect. **Figures 13** and **14** show the results of multiple comparisons with respect to electrode size and channel number, respectively. The above results indicate that enlarging electrode size or increasing stimulation channel cannot change the temporal variation of MFCV.

**Table 6.** The four NMF features for all 5 subjects.

	$CR_{MNF}$ (0–50)% (Hz/s)	$CR_{MNF}$ (50–75)% (Hz/s)	$RC_{MNF}$ (0–50)% (%)	$RC_{MNF}$ (0–75)% (%)
SCES	$-0.20 \pm 0.20$	$-0.13 \pm 0.11$	$-5.8\% \pm 6.9\%$	$-9.1\% \pm 14.9\%$
SSES	$-0.08 \pm 0.19$	$-0.06 \pm 0.20$	$-1.4\% \pm 29.8\%$	$-9.9\% \pm 28.2\%$
DCES	$-0.03 \pm 0.02$	$-0.01 \pm 0.02$	$-5.1\% \pm 8.8\%$	$-5.3\% \pm 6.9\%$
TCES	$-0.06 \pm 0.09$	$-0.03 \pm 0.02$	$-9.1\% \pm 27.1\%$	$-15.1\% \pm 17.9\%$

**Table 7.** Results of two-factor ANOVA analysis.

	<i>P</i> -value		$\eta^2$	
	Configuration	Subject	Configuration	Subject
$CR_{MNF}$ (0–50)%	0.904	0.975	0.020	0.085
$CR_{MNF}$ (50–75)%	0.720	0.712	0.048	0.187
$RC_{MNF}$ (0–50)%	0.105	0.748	0.200	0.177
$RC_{MNF}$ (0–75)%	0.178	0.752	0.184	0.176

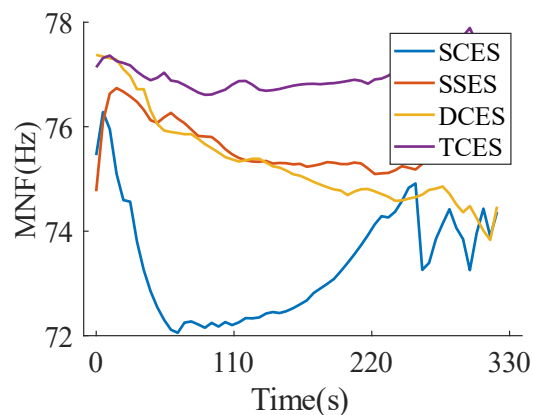


**Figure 12.** MNF curve of a representative subject.

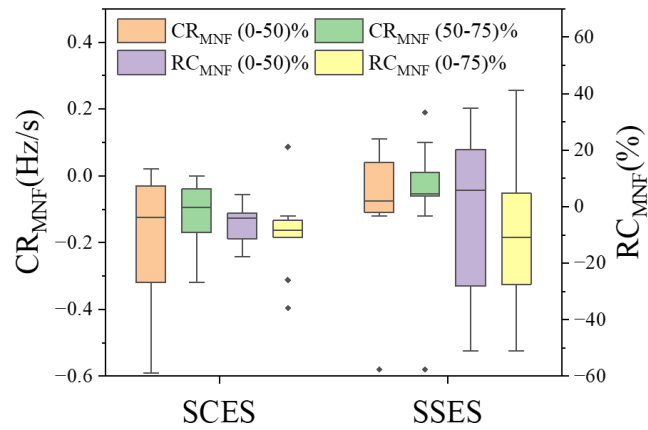


**Figure 13.** Multiple comparison regarding electrode size. ♦ Denotes outliers.

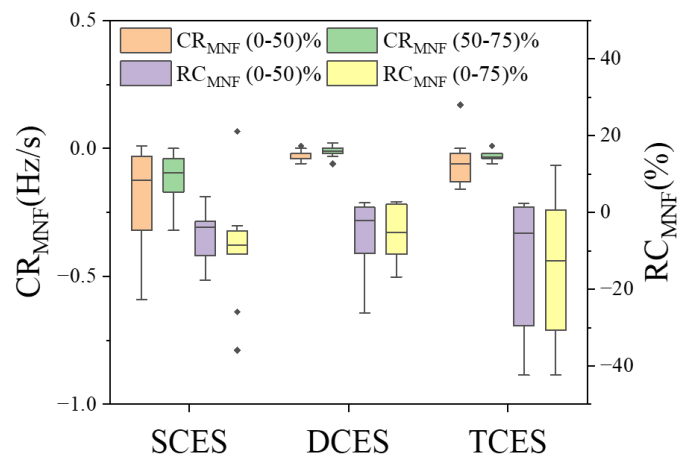


**Figure 14.** Multiple comparison regarding channel number. ♦ Denotes outliers.

### 3.3. Analysis of recruitment property of type I MU

For the signal collected under 1 Hz low-frequency stimulation, the selected feature is M-PA. The higher the M-PA value, the more the recruited Type I MUs. **Figure 15** shows the M-PA curve of a representative subject in the first 5.5 min of FES experiments with the four electrode configurations. For all four electrode configurations, M-PA changes slightly with the stimulation time and remains stable at last. It indicates that Type I MUs recruited under low-frequency FES are insensitive to stimulation time. However, there are significant differences ( $p > 0.05$ ) in M-PA under different electrode configurations, namely  $SSES > TCES > DCES > SCES$ . The aM-PA value for SSES is 1.75, significantly higher than those of 1.29, 1.51, and 1.57 for TCES, DCES, and SCES, respectively; post-hoc power analysis indicated that the statistical power exceeded 0.8. The results showed that under 1 Hz stimulation, compared with increasing the number of stimulation channels, enlarging electrode size can more effectively enhance Type I MU recruitment ability.

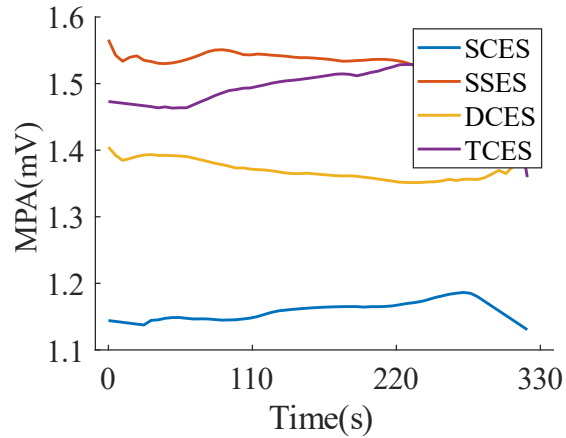


**Figure 15.** MPA curve of a representative subject.

**Table 8** records the average  $CR_{M-PA}$  and  $RC_{M-PA}$  for all ten subjects and **Table 9** shows the results of the two-factor analysis. **Figures 16** and **17** show the results of  $CR_{M-PA}$  and  $RC_{M-PA}$  of multiple comparisons with respect to electrode size and channel number. There was no significant difference ( $p > 0.05$ ) in  $CR_{M-PA}$  and  $RC_{M-PA}$  among the four configurations. This suggests that, under low-frequency stimulation, neither enlarging the electrode size nor increasing the stimulation channel can change the temporal variation of Type I MU recruitment property.

**Table 8.** Average features related to M-wave for all ten subjects.

	$CR_{M-PA}$ (0–50)% ( $\mu V/s$ )	$CR_{M-PA}$ (50–75)% ( $\mu V/s$ )	$RC_{M-PA}$ (0–50)% (%)	$RC_{M-PA}$ (0–75)% (%)	aM-PA (mV)
SCES	$-0.83 \pm 4.62$	$0.49 \pm 3.43$	$1.4\% \pm 15.5\%$	$6.3\% \pm 18.3\%$	$1.29 \pm 0.61$
SSES	$1.21 \pm 1.57$	$1.35 \pm 0.75$	$11.2\% \pm 11.3\%$	$16.2\% \pm 12.3\%$	$1.75 \pm 0.43$
DCES	$0.09 \pm 0.88$	$-0.06 \pm 0.77$	$1.2\% \pm 7.7\%$	$-0.2\% \pm 9.2\%$	$1.51 \pm 0.70$
TCES	$1.04 \pm 0.63$	$1.57 \pm 0.48$	$16.8\% \pm 12.3\%$	$20.2\% \pm 21.5\%$	$1.57 \pm 0.48$

**Table 9.** Results of two-factor ANOVA analysis.

	<i>P</i> -value		$\eta^2$	
	Configuration	Subject	Configuration	Subject
$CR_{M-PA}$ (0–50)%	0.059	0.637	0.304	0.206
$CR_{M-PA}$ (50–75)%	0.228	0.230	0.292	0.321
$RC_{M-PA}$ (0–50)%	0.123	0.559	0.190	0.226
$RC_{M-PA}$ (0–75)%	0.374	0.690	0.107	0.193
aM-PA	0.028	0.922	0.281	0.119

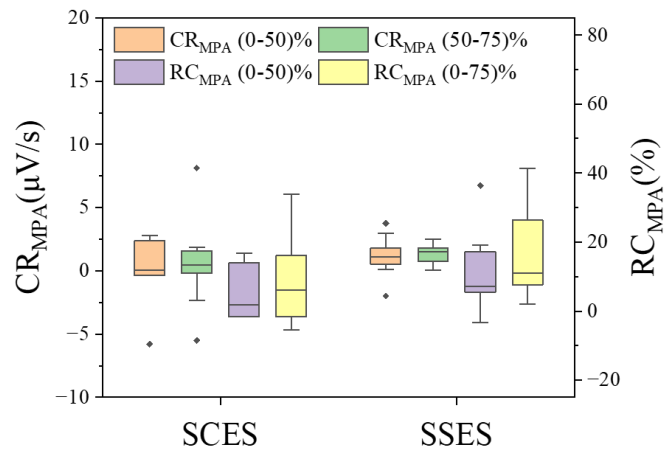


**Figure 16.** Multiple comparison regarding electrode size. ♦ Denotes outliers.

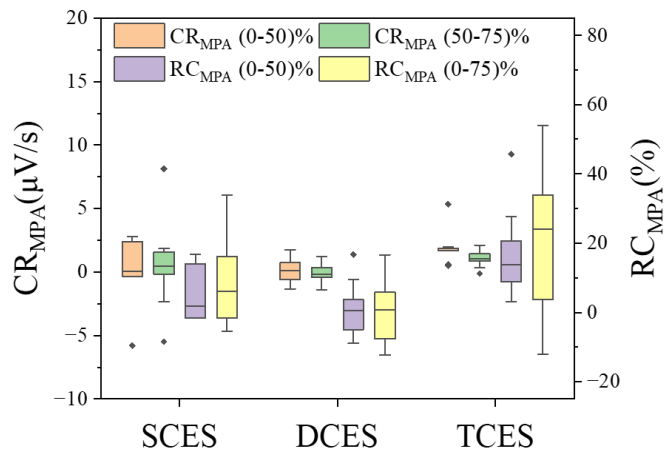


**Figure 17.** Multiple comparison regarding channel number. ♦ Denotes outliers.

## 4. Discussion

Taking the biceps brachii as the target muscle, this study investigates the effect of different stimulation electrode size and stimulation channel on muscle contraction strength and myoelectric activity. In summary, both enlarging the electrode size and increasing the stimulation channel can delay muscle fatigue and enhance motor unit recruitment with minimal impact on the changes over time in MFCV and Type I MU. Enlarging the electrode size is more conducive to recruiting more MUs and enhancing muscle contraction output, while increasing the number of stimulation channels is more conducive to delaying muscle fatigue effects. The findings can provide valuable insights for developing clinical FES rehabilitation protocols. The discussion is as follows.

### 4.1. Possible choices for high/low intensity stimulation

The effectiveness of FES treatment is often considered to be proportional to the extent of muscle contraction it induces. For training the ability of muscle contraction, a certain threshold of force must typically be achieved for effective FES treatment [8,31]. Theoretically, higher current intensity results in better outcomes because higher current intensity can induce stronger depolarization, leading to more powerful muscle

contractions. However, excessively high current intensity may lead to antidromic transmission, blocking impulses emanating from the spinal motor neuron pool and thus reducing the overall rehabilitation effect. Furthermore, stimulation intensity directly affects patient comfort and higher currents often result in worse tolerance. Therefore, determining the optimal stimulation intensity is crucial for FES treatment.

In this study, we compared the FES effects of a 4.9 cm<sup>2</sup> circular small electrode and a 10 cm<sup>2</sup> square large electrode on the biceps brachii under the same stimulation current intensity. The results showed that the 10 cm<sup>2</sup> large electrode significantly improved muscle force output, suggesting that a larger electrode can enhance muscle contraction strength. Based on these results, it is recommended to consider using larger electrodes for low-intensity FES treatment in patients with poor tolerance. Additionally, the study also compared the effects of single-channel, dual-channel, and triple-channel stimulation. The results indicated that increasing the number of stimulation channels can induce muscle contraction at lower current intensities and significantly improve muscle strength output. Therefore, increasing the number of stimulation channels can improve patient tolerance in high-intensity FES treatments, especially for hyper-sensitive patients or those with low bone density. For these patients, it is recommended to use two or more electrodes on a single muscle during FES treatment, thereby reducing the absolute current intensity per channel. This approach decreases the stimulation load on the skin, muscles, and other tissues, minimizing side effects such as muscle discomfort and muscle spasms that may result from excessively high stimulation intensity.

#### **4.2. Potential strategies for enhancing FES effectiveness**

The effects of FES on the target muscle can be analyzed from the perspectives of muscle contraction strength and myoelectric activity. This study found that enlarging electrode size and increasing the number of stimulation channels can effectively enhance muscle contraction strength, delay muscle fatigue progress, and increase the recruitment of Type II motor units, thereby improving FES treatment effect. However, the specific differences in the effects of enlarging electrode size versus increasing the number of stimulation channels are worth considering and should be chosen based on the particular needs of the patient.

Firstly, electrical stimulation typically leads to rapid muscle fatigue, resulting in decreased muscle contraction strength, which limits FES effectiveness. Our research has shown that both enlarging electrode size and increasing the number of stimulation channels significantly can delay muscle fatigue progress. However, increasing more stimulation channels cannot further delay fatigue progress or significantly improve force output after rapid fatigue. On the other hand, enlarging electrode size can effectively improve muscle force output during the initial phase of stimulation. Therefore, for treatments requiring prolonged stimulation or targeting fatigue-sensitive rehabilitation, increasing the number of stimulation channels can help mitigate the effects of muscle fatigue. Conversely, for tasks requiring high muscle force output within a short time, particularly in exercise training, enlarging electrode size is a good selection. For weightlifters or mountaineers, we recommend using a single electrode larger than 10 cm<sup>2</sup> to target large muscle groups, such as the biceps.

Furthermore, FES should not be used for more than 10 min at a time due to muscle fatigue.

Secondly, muscle contraction strength is closely related to MU recruitment. Theoretically, the more MUs recruited, the better the FES treatment effect. Low-frequency stimulation primarily recruits Type I MU, while high-frequency stimulation is more effective at recruiting Type II MU. Some studies also suggest that electrical stimulation can alter muscle fiber composition, converting Type II fibers into Type I fibers [41]. To investigate the effects of enlarging electrode size and increasing the number of stimulation channels on the recruitment of different types of MUs, our research designed an alternating high-low frequency stimulation protocol. The results indicate that Type I and Type II motor units have different sensitivities to electrical stimulation, which is consistent with the viewpoint of Vromans et al. that muscles composed of different muscle fibers have different sensitivities to stimulation frequencies [19].

The analysis of Type II motor unit recruitment under 30 Hz high-frequency stimulation found that both increasing electrode size and the number of stimulation channels can effectively improve MU recruitment level, thereby enhancing FES effectiveness. Since the electric field rapidly decays as the distance between the electrodes (anode and cathode) increases, single-channel or small-size electrodes may not deliver enough current to activate the widespread neural branches within the muscle [17]. Enlarging electrode size and increasing the number of stimulation channels provide a broader electric field distribution, activating more neural branches and recruiting more Type II MUs while the recruitment capacity and MFCV remain relatively stable, with little variation over time. Compared to SSES, DCES, or TCES, recruits fewer MUs, which may be due to the current intensity in each channel being only half or one-third that of single-channel stimulation. Nevertheless, the type II MU recruitment capacity of TCES approaches that of SSES, and DCES is close to that of SCES. The recruitment capacity of multi-channel stimulation remains stable over time, while that of SSES significantly declines over time. Therefore, for high-frequency FES therapy (20–50 Hz) aimed at improving muscle strength, multi-channel stimulation seems to be a better option. For patients with motor dysfunction requiring rehabilitation of the upper limb muscles, a rehabilitation session typically lasts 20–30 min [42]. It is essential to both adequately stimulate the muscles and prolong the time to fatigue. So for large muscles, such as the biceps, multiple electrodes smaller than 5 cm<sup>2</sup> should be used to ensure effective stimulation.

The analysis of Type I MU recruitment under 1 Hz low-frequency stimulation also showed that both enlarging electrode size and increasing the number of channels can enhance motor unit recruitment, thus improving FES effectiveness. Compared to increasing the number of channels, enlarging electrode size is more effective in enhancing the recruitment of Type I MUs. Additionally, because Type I fibers contain more mitochondria [43], their recruitment capacity is more stable compared to Type II fibers, with only a slight increase over time, and finally remains stable. This phenomenon suggests that enlarging the electrode size or increasing the number of channels can significantly enhance the activation of Type I fibers, which is crucial for long-term rehabilitation, muscle endurance training, and the treatment of muscle atrophy in elderly populations. Therefore, for the treatment of long-term (30 min–1

day) low-frequency FES (1–20 Hz) aimed at preventing muscle atrophy and improving muscle endurance and venous blood flow [3,4,29], the electrode area can be appropriately increased to improve the therapeutic effect. We recommend using a single electrode with an area larger than 10 cm<sup>2</sup> for FES treatment, as this ensures both efficacy and long-term stability of electrode placement.

## 5. Conclusion

The main contribution of this study is to investigate the impact of enlarging electrode size and increasing the number of stimulation channels on the effectiveness of FES from the perspectives of muscle contraction strength and myoelectric activity. The research results demonstrate that enlarging electrode size and increasing stimulation channels can delay muscle fatigue, enhance motor unit recruitment, and generate stronger muscle contraction at the same current intensity. Additionally, different types of motor units exhibit varying sensitivities to electrical stimulation. These findings provide valuable insights for clinicians, enabling the adjustment of electrode size and stimulation channel numbers according to individual patient needs, ultimately improving the therapeutic efficacy of FES.

The limitation of this study is that FES experiments and data analysis were performed on the biceps of only 10 healthy subjects. However, the fiber composition and function of different muscles vary in response to FES, and studying the biceps alone cannot fully reflect the impact of other muscles on FES. In addition, there are significant differences in muscle reactivity and functional recovery between healthy individuals and those with neuromuscular disease, which limits the clinical application of the findings. In order to overcome these limitations, future studies will explore the effects of different electrode configurations in FES on various muscles and its mechanisms in rehabilitation therapy for patients with motor impairments.

**Ethical approval:** The study was conducted in accordance with the Declaration of Helsinki, and approved by Biomedical Ethics Committee of the University of Science and Technology of China (No. 2022-N(H)-150).

**Conflict of interest:** The author declares no conflict of interest.

## Abbreviations

FES	Functional electrical stimulation
MU	motion unit
sEMG	surface electromyography
MFCV	muscle fiber conduction velocity
eEMG	evoked electromyography
MVC	maximum voluntary contraction
APB	abductor pollicis brevis
VL	vastus lateralis
SDSS	spatially distribute sequential stimulation
SES	single electrode stimulation
SRE	small round electrode

LSE	large square electrode
SCES	single-channel round electrode scheme
SSES	single-channel square electrode scheme
DCES	dual-channel round electrode scheme
TCES	triple-channel round electrode scheme
ICF	isometric contraction force
MIC	maximum isometric contractions
FT	fatigue time
FTI	fatigue time integral
RMS	root mean square
MNF	mean frequency
M-PA	positive amplitude of M-wave
ANOVA	Analysis of Variance

## References

1. Aout T, Begon M, Jegou B, et al. Effects of Functional Electrical Stimulation on Gait Characteristics in Healthy Individuals: A Systematic Review. *Sensors*. 2023; 23(21): 8684. doi: 10.3390/s23218684
2. Schardong J, Kuinchtner GC, Sbruzzi G, et al. Functional electrical stimulation improves muscle strength and endurance in patients after cardiac surgery: a randomized controlled trial. *Brazilian Journal of Physical Therapy*. 2017; 21(4): 268-273. doi: 10.1016/j.bjpt.2017.05.004
3. Miyamoto T, Kamada H, Tamaki A, et al. Low-intensity electrical muscle stimulation induces significant increases in muscle strength and cardiorespiratory fitness. *European Journal of Sport Science*. 2016; 16(8): 1104-1110. doi: 10.1080/17461391.2016.1151944
4. Allen CB, Williamson TK, Norwood SM, et al. Do Electrical Stimulation Devices Reduce Pain and Improve Function?—A Comparative Review. *Pain and Therapy*. 2023; 12(6): 1339-1354. doi: 10.1007/s40122-023-00554-6
5. Purohit R, Varas-Diaz G, Bhatt T. Functional electrical stimulation to enhance reactive balance among people with hemiparetic stroke. *Experimental Brain Research*. 2024; 242(3): 559-570. doi: 10.1007/s00221-023-06729-z
6. Kern H, Boncompagni S, Rossini K, et al. Long-Term Denervation in Humans Causes Degeneration of Both Contractile and Excitation-Contraction Coupling Apparatus, Which Is Reversible by Functional Electrical Stimulation (FES): A Role for Myofiber Regeneration? *Journal of Neuro pathology & Experimental Neurology*. 2004; 63(9): 919-931. doi: 10.1093/jnen/63.9.919
7. Popovic MR, Masani K, Milosevic M. Functional Electrical Stimulation Therapy: Mechanisms for Recovery of Function Following Spinal Cord Injury and Stroke. In: *Neurorehabilitation Technology*. Springer International Publishing: Cham; 2022.
8. Bergquist AJ, Clair JM, Lagerquist O, et al. Neuromuscular electrical stimulation: implications of the electrically evoked sensory volley. *European Journal of Applied Physiology*. 2011; 111(10): 2409-2426. doi: 10.1007/s00421-011-2087-9
9. Scott WB, Binder-Macleod SA. Changing stimulation patterns improves performance during electrically elicited contractions. *Muscle & Nerve*. 2003; 28(2): 174-180. doi: 10.1002/mus.10412
10. Taylor JL, Amann M, Duchateau J, et al. Neural Contributions to Muscle Fatigue. *Medicine & Science in Sports & Exercise*. 2016; 48(11): 2294-2306. doi: 10.1249/mss.0000000000000923
11. Chou LW, Binder-Macleod SA. The effects of stimulation frequency and fatigue on the force–intensity relationship for human skeletal muscle. *Clinical Neurophysiology*. 2007; 118(6): 1387-1396. doi: 10.1016/j.clinph.2007.02.028
12. Enoka RM, Duchateau J. Muscle fatigue: what, why and how it influences muscle function. *The Journal of Physiology*. 2008; 586(1): 11-23. doi: 10.1113/jphysiol.2007.139477
13. Estigoni EH, Fornusek C, Smith RM, et al. Evoked EMG and Muscle Fatigue During Isokinetic FES-Cycling in Individuals With SCI. *Neuromodulation: Technology at the Neural Interface*. 2011; 14(4): 349-355. doi: 10.1111/j.1525-1403.2011.00354.x

14. De Marchis C, Santos Monteiro T, Simon-Martinez C, et al. Multi-contact functional electrical stimulation for hand opening: electrophysiologically driven identification of the optimal stimulation site. *Journal of NeuroEngineering and Rehabilitation*. 2016; 13(1). doi: 10.1186/s12984-016-0129-6
15. Li Z, Guiraud D, Andreu D, et al. Real-Time Closed-Loop Functional Electrical Stimulation Control of Muscle Activation with Evoked Electromyography Feedback for Spinal Cord Injured Patients. *International Journal of Neural Systems*. 2018; 28(06): 1750063. doi: 10.1142/s0129065717500630
16. Murakami K, Fujisawa H, Onobe J, et al. Relationship between Muscle Fiber Conduction Velocity and the Force-time Curve during Muscle Twitches. *Journal of Physical Therapy Science*. 2014; 26(4): 621-624. doi: 10.1589/jpts.26.621
17. Buckmire AJ, Arakeri TJ, Reinhard JP, et al. Mitigation of excessive fatigue associated with functional electrical stimulation. *Journal of Neural Engineering*. 2018; 15(6): 066004. doi: 10.1088/1741-2552/aade1c
18. Gorgey AS, Mahoney E, Kendall T, et al. Effects of neuromuscular electrical stimulation parameters on specific tension. *European Journal of Applied Physiology*. 2006; 97(6): 737-744. doi: 10.1007/s00421-006-0232-7
19. Vromans M, Faghri PD. Functional electrical stimulation-induced muscular fatigue: Effect of fiber composition and stimulation frequency on rate of fatigue development. *Journal of Electromyography and Kinesiology*. 2018; 38: 67-72. doi: 10.1016/j.jelekin.2017.11.006
20. RaviChandran N, Teo MY, Aw K, et al. Design of Transcutaneous Stimulation Electrodes for Wearable Neuroprostheses. *IEEE Transactions on Neural Systems and Rehabilitation Engineering*. 2020; 28(7): 1651-1660. doi: 10.1109/tnsre.2020.2994900
21. Bickel CS, Gregory CM, Dean JC. Motor unit recruitment during neuromuscular electrical stimulation: a critical appraisal. *European Journal of Applied Physiology*. 2011; 111(10): 2399-2407. doi: 10.1007/s00421-011-2128-4
22. Sayenko DG, Nguyen R, Popovic MR, et al. Reducing muscle fatigue during transcutaneous neuromuscular electrical stimulation by spatially and sequentially distributing electrical stimulation sources. *European Journal of Applied Physiology*. 2014; 114(4): 793-804. doi: 10.1007/s00421-013-2807-4
23. Nguyen R, Masani K, Micera S, et al. Spatially Distributed Sequential Stimulation Reduces Fatigue in Paralyzed Triceps Surae Muscles: A Case Study. *Artificial Organs*. 2011; 35(12): 1174-1180. doi: 10.1111/j.1525-1594.2010.01195.x
24. Ye G, Theventhiran P, Masani K. Effect of Spatially Distributed Sequential Stimulation on Fatigue in Functional Electrical Stimulation Rowing. *IEEE Transactions on Neural Systems and Rehabilitation Engineering*. 2022; 30: 999-1008. doi: 10.1109/tnsre.2022.3166710
25. Flodin J, Juthberg R, Ackermann PW. Effects of electrode size and placement on comfort and efficiency during low-intensity neuromuscular electrical stimulation of quadriceps, hamstrings and gluteal muscles. *BMC Sports Science, Medicine and Rehabilitation*. 2022; 14(1). doi: 10.1186/s13102-022-00403-7
26. Lu C, Ge R, Tang Z, et al. Multi-Channel FES Gait Rehabilitation Assistance System Based on Adaptive sEMG Modulation. *IEEE Transactions on Neural Systems and Rehabilitation Engineering*. 2023; 31: 3652-3663. doi: 10.1109/tnsre.2023.3313617
27. Mooney JA, Rose J. A Scoping Review of Neuromuscular Electrical Stimulation to Improve Gait in Cerebral Palsy: The Arc of Progress and Future Strategies. *Frontiers in Neurology*. 2019; 10. doi: 10.3389/fneur.2019.00887
28. Veldman MP, Gondin J, Place N, et al. Effects of Neuromuscular Electrical Stimulation Training on Endurance Performance. *Frontiers in Physiology*. 2016; 7. doi: 10.3389/fphys.2016.00544
29. Wainwright TW, Burgess LC, Middleton RG. A feasibility randomised controlled trial to evaluate the effectiveness of a novel neuromuscular electro-stimulation device in preventing the formation of oedema following total hip replacement surgery. *Heliyon*. 2018; 4(7): e00697. doi: 10.1016/j.heliyon.2018.e00697
30. Calbiyik M, Yilmaz S. Role of Neuromuscular Electrical Stimulation in Increasing Femoral Venous Blood Flow After Total Hip Prosthesis. *Cureus*. 2022; 14(9): e29255. doi: 10.7759/cureus.29255
31. Dreibati B, Lavet C, Pinti A, et al. Influence of electrical stimulation frequency on skeletal muscle force and fatigue. *Annals of Physical and Rehabilitation Medicine*. 2010; 53(4): 266-277. doi: 10.1016/j.rehab.2010.03.004
32. Polgar J, Johnson MA, Weightman D, Appleton D. Data on fibre size in thirty-six human muscles: An autopsy study. *Journal of the Neurological Sciences*. 1973; 19(3): 307-318. doi: 10.1016/0022-510X(73)90094-4
33. Korhonen RJ, Hernandez-Pavon JC, Metsomaa J, et al. Removal of large muscle artifacts from transcranial magnetic stimulation-evoked EEG by independent component analysis. *Medical & Biological Engineering & Computing*. 2011; 49(4): 397-407. doi: 10.1007/s11517-011-0748-9

34. Girard O, Bishop DJ, Racinais S. M-wave normalization of EMG signal to investigate heat stress and fatigue. *Journal of Science and Medicine in Sport*. 2018; 21(5): 518-524. doi: 10.1016/j.jsams.2017.07.020
35. De Luca CJ. The Use of Surface Electromyography in Biomechanics. *Journal of Applied Biomechanics*. 1997; 13(2): 135-163. doi: 10.1123/jab.13.2.135
36. Lowery M, Nolan P, O'Malley M. Electromyogram median frequency, spectral compression and muscle fibre conduction velocity during sustained sub-maximal contraction of the brachioradialis muscle. *Journal of Electromyography and Kinesiology*. 2002; 12(2): 111-118. doi: 10.1016/S1050-6411(02)00004-4
37. Orizio C. Soundmyogram and EMG cross-spectrum during exhausting isometric contractions in humans. *Journal of Electromyography and Kinesiology*. 1992; 2(3): 141-149. doi: 10.1016/1050-6411(92)90011-7
38. de Sousa ACC, Valtin M, Bó APL, et al. Automatic Detection of Stimulation Artifacts to Isolate Volitional from Evoked EMG Activity. *IFAC-PapersOnLine*. 2018; 51(27): 282-287. doi: 10.1016/j.ifacol.2018.11.628
39. Rodriguez-Falces J, Place N. Determinants, analysis and interpretation of the muscle compound action potential (M wave) in humans: implications for the study of muscle fatigue. *European Journal of Applied Physiology*. 2017; 118(3): 501-521. doi: 10.1007/s00421-017-3788-5
40. Rodriguez-Falces J, Place N. Differences in the recruitment curves obtained with monopolar and bipolar electrode configurations in the quadriceps femoris. *Muscle & Nerve*. 2016; 54(1): 118-131. doi: 10.1002/mus.25006
41. Chu X, Sun J, Liang J, et al. Mechanisms of muscle repair after peripheral nerve injury by electrical stimulation combined with blood flow restriction training. *Sports Medicine and Health Science*. 2025; 7(3): 173-184. doi: 10.1016/j.smhs.2024.10.002
42. Xue J, Kong H, Liao M, et al. Effects of Functional Electrical Stimulation Based on Walking Pattern with Different Treatment Time on Lower Limb Function in Stroke Patients: A Randomized Controlled Study. *Rehabilitation Medicine*. 2022; 32(1): 25-31. doi: 10.3724/sp.j.1329.2022.01005
43. Dong H, Tsai SY. Mitochondrial Properties in Skeletal Muscle Fiber. *Cells*. 2023; 12(17): 2183. doi: 10.3390/cells12172183